Isı Bilimi ve Tekniği Dergisi, 34, 1, 43-51, 2014
J. of Thermal Science and Technology
©2014 TIBTD Printed in Turkey
ISSN 1300-3615

ENERGY EVALUATION OF A PHASE CHANGE MATERIAL WALL COVERED WITH NOVEL TRIPLE GLASS

Aslıhan KURNUÇ* ve Yusuf Ali KARA**

*Mechanical Engineering Department, Faculty of Engineering, Erzincan University, 24100 Erzincan, Turkey, akurnuc@erzincan.edu.tr

**Mechanical Engineering Department, Faculty of Engineering, Ataturk University, 25100 Erzurum, Turkey, yalikara@atauni.edu.tr

(Geliş Tarihi: 08.05.2012 Kabul Tarihi: 23.10.2012)

Abstract: A research study was conducted to investigate the thermal performance of phase change material (PCM) walls. The south-facing external wall of a test room was constructed using PCM walls composed of brick walls, plasterboards containing PCMs, and novel triple glass. The thermal performance of the PCM walls was experimentally determined on a monthly basis. However, because of the unstable characteristic of the meteorological data, evaluation of any solar application is usually made using the mean values from long-term meteorological data. In addition to the experimental analysis, a theoretical performance analysis based on 10-year mean meteorological data was carried out to provide a more general conclusion about the performance of the PCM walls. The results from the theoretical analysis show that the ratio of the solar energy gain provided by the GR35 PCM wall to the heat load of the test room on a monthly basis varies from 7 to 57% during the heating period from October to May; the ratio is 16% on an annual basis.
Keywords: Phase change material (PCM), Solar space heating, PCM wall, PCM Trombe wall

YENİ TASARI ÜÇLÜ CAMLI FAZ DEĞİŞİM MADDELİ DUVARIN ENERJİ DEĞERLENDİRMESİ

Özet: Bu çalışma faz değişim maddeli duvarın ısıl performansını araştırmak amacıyla yapılmıştır. Deney odasının güney cephesi tuğla duvar, faz değişim maddesi içeren sıva levhası ve yeni tasarı üçlü cam bileşenlerinden oluşan faz değişim maddeli duvar kullanılarak inşa edilmiştir. FDM duvarın ısıl performansı aylık bazda deneysel olarak saptanmıştır. Ancak, meteorolojik verilerin değişken karakteristikli olması sebebiyle herhangi bir güneş uygulamasının değerlendirmesi genellikle uzun dönemlik meteorolojik verilerden oluşturulan ortalama değerler kullanılarak yapılır. FDM duvarın performansı hakkında daha genel bir sonuç elde etmek için deneysel analize ek olarak on yıllık ortalama meteorolojik verilere dayanan teorik performans analizi gerçekleştirilmiştir. Teorik analizden elde edilen sonuçlar deney odasının ısıtma yükünün GR35 FDM duvar tarafından sağlanan güneş enerjisi kazanım oranının Ekim ayından Mayıs ayına kadar olan ısıtma periyodu süresince aylık bazda %7'den %57'ye kadar değiştiği ve yıllık bazda ise %16 olduğunu göstermektedir.
Anahtar Kelimeler: Faz değişim maddesi (FDM), Güneşle boşluk ısıtma, FDM duvar, FDM Trombe duvar

NOMENCLATURE

Symbols

A	area [m^2]
c_p	specific heat [W/kg·K]
E	energy [J]
f	correction factor for heat gains
g	solar transmittance
H	specific heat loss [W/K]
$\bar{H}$	monthly mean daily radiation [J/m^2-day]
I	characteristic length of the heat bridge [m]
k	thermal conductivity [W/m·K]
$\dot{m}$	mass flow rate [kg/s]
N	day number of a month
n	number of air change
$\dot{Q}$	heat rate [W]
r	diffuse reflectance of surroundings
$\bar{R}$	ratio of average daily beam radiation on the tilted surface to that on a horizontal surface for the month
t	time [s]
T	temperature [K]
U	overall heat transfer coefficient [W/m^2·K]
V	ventilated volume [m^3], velocity [m/s]
β	slope angle
δ	declination angle

η	efficiency
ρ	density
ϕ	latitude
ω	sunset hour angle

Subscripts

a	air
b	beam
c	cross-section, conduction
d	daily, diffuse, duct
f	fuel
g	Gain
h	heat load
lv	lower vent
i	incident, inside, indoor
m	monthly, mean
o	overall, outdoor
s	surface, sunset, solar
T, *t*	tilt, transmit
uv	upper vent
v	ventilation

Abbreviations

DSC	differential scanning calorimetry
NTG	novel triple glass
PCM	phase change material
SEG	solar energy gain
RSEG	ratio of solar energy gain
ST	solar transmittance

INTRODUCTION

Latent heat storage in phase change materials (PCMs) is an efficient way to store thermal energy because PCMs have a high-energy storage density over a narrow temperature range. Solar energy can be absorbed and stored in the building envelope by incorporating PCMs into the walls, ceilings, floors, and windows of the building.

The following related topics have been reviewed and discussed by different researchers: the basic principles of storing solar energy by incorporating PCMs into building envelopes; the thermophysical properties of candidate PCMs for building applications; the methods of PCM encapsulation; the methods of PCM incorporation into building envelopes; thermal analyses of PCM-enhanced walls, ceilings, and floors; the effect of PCM inclusion in the building envelope on the thermal performance of the building; and manufacturing methods for producing PCM-enhanced wallboards, concrete, and building insulation materials (Hauer et al., 2002; Khudhair and Farid, 2004; Zhang et al., 2007; Tyagi and Buddhi, 2007; Pasupathy et al., 2008; Sharma et al., 2009; Baetens et al., 2010).

Chan (2011) developed a theoretical model to investigate the thermal performance of a flat with PCM-incorporated external walls. It was reported that the external PCM walls provided an energy savings of 2.9% by reducing the need to use the air conditioning system in the flat. Diaconu and Cruceru (2010) proposed a three-layer composite wall system. The external and internal layers of the composite wall were PCM wallboards impregnated with different PCMs, and the middle layer was a thermal insulation panel. The melting point of the PCM in the external layer was higher than that in the internal layer. An annual simulation for a room constructed with a composite wall system was carried out, and it was found that the composite wall system reduced the peak value of cooling/heating loads of the room and provided energy saving. Zhang et al. (2011) developed a model based on an enthalpy-porosity technique to investigate the thermal response of brick walls filled with PCM. They found that the use of PCM in brick walls was beneficial for thermal insulation, temperature hysteresis, and thermal comfort.

Kuznik et al. (2011) investigated the thermal performance of PCM wallboards by monitoring two identical rooms. One of the rooms had PCM wallboards placed on the internal surfaces of the walls and the ceiling. Comparing the indoor air temperatures and the wall surface temperatures of the rooms, they inferred that PCM wallboards enhanced the thermal comfort of occupants. Cerón et al. (2011) developed and designed a new prototype of tile including PCM. The PCM tiles consisted of clay stoneware, a top metal sheet, a metal container containing the PCM, and a thermal insulation layer. They placed the PCM tiles on the floor of a test room receiving solar radiation. They found that during the day, the surface temperature of the PCM tiles was slightly (1–2ºC) higher than that of tiles without PCM. They concluded that the PCM tiles placed on the floor decreased heat loss through the floor during the winter and could be used as passive thermal conditioners in a house to stabilise the room temperature.

Liu and Awbi (2009) tested the thermal performance of a test room with PCM wallboards under natural convection. They placed the PCM wallboards on the inner surface of the room's wall. They found that PCM wallboards reduced the heat flux density and the interior wall surface temperature during the charging process, and the heat insulation performance of the PCM wall was better than that of an ordinary wall. Castellón et al. (2010) investigated the thermal performance of sandwich panels including microencapsulated PCM. They added the microencapsulated PCM to the sandwich panels to increase their thermal inertia.

Cabeza et al. (2007) built two identical concrete cubicles as test rooms; one was constructed using PCM-enhanced concrete, and the other one was constructed using conventional concrete without PCM. A commercial microencapsulated PCM with a melting point of 26 ºC was used in the concrete. The results of the study showed that the PCM-enhanced concrete cubicle had a better thermal mass and a lower inner temperature compared with the conventional concrete cubicle. Castell et al. (2010) constructed several test chambers using two types of brick walls integrated with PCM and an identical reference chamber without PCM to compare the chambers' thermal performance under real conditions. They monitored the temperature of the walls, the indoor air temperature of the chambers, and the heat flux entering through the south wall. They performed the tests both with and without an air conditioner. They found that the PCM could reduce the peak temperatures up to 1 ºC and smooth temperature fluctuations. Furthermore, a 15% energy savings was achieved in the PCM chambers.

A shape-stabilised PCM is a compound material made of PCMs and supporting materials (usually high-density polyethylene). The shape-stabilised PCM keeps its form unchanged during the phase change process. The preparation methods and thermophysical properties of shape-stabilised PCMs were given by Zhang et al. (2006). Some applications of shape-stabilised PCM panels in buildings were studied both experimentally and numerically by different researchers (Lin et al., 2004; Lin et al., 2005; Zhou et al., 2007; Zhou et al., 2008). More than half of the total electric energy consumption of a room can be shifted from the peak period to the off-peak period by combining an under-floor electric heating system with shape-stabilised PCM panels (Lin et al., 2004; Lin et al., 2005). The shape-stabilised PCM plates improve indoor thermal comfort and eliminate approximately 47% of normal and peak-hour energy use and 12% of energy consumption in winter when they are placed on the interior surface of the walls and the ceiling of a room as inner linings (Zhou et al., 2007; Zhou et al., 2008).

A test room with PCM walls made of brick walls, plasterboards containing PCMs, and novel triple glass (NTG) was constructed to investigate the thermal performance of the PCM walls in Erzurum, Turkey. The test room was monitored over a one-year period. The experimental data were analysed on a monthly basis to calculate overall conversion efficiency of the PCM walls. The performance analysis of the NTG-PCM wall system on a monthly basis was previously presented for the experimental period from October 2008 to October 2009 (Kara and Kurnuç, 2012a; Kara and Kurnuç, 2012b). However, because the performance analysis in Ref. (Kara and Kurnuç, 2012b) was evaluated on a monthly basis, it was strongly dependant on the number of sunny days in the month. Because the number of sunny days in a month varies from year to year, the performance parameters such as the solar energy gain (SEG), the ratio of the solar energy gain (RSEG) provided by the PCM walls to the heat load, which indicates the fraction of the heat load provided by the PCM walls, were valid only for the experimental period (Kara and Kurnuç, 2012b). Therefore, general conclusions could not be drawn by considering the SEG or RSEGs presented in (Kara and Kurnuç, 2012b). In this study, a theoretical energy analysis on a monthly basis was carried out by using 10-year mean meteorological data, and the following parameters were regenerated to provide a more general conclusion about the performance of the PCM walls: solar radiation incident on the PCM walls, solar energy gain (SEG) provided by the PCM walls, heat load of the test room, and ratio of the solar energy gain (RSEG) provided by the PCM walls to the heat load. Besides, the experimental evaluations given in Ref. (Kara and Kurnuç, 2012b) are briefly presented in the current work for the reader convenience.

MATERIAL AND METHODS

Experimental Work

The layout of the test room is shown in Fig. 1. There were two PCM walls on either side of the south façade with a window between them, as shown in Fig. 1. The structures of the PCM walls were the same; however, different PCMs were used. The PCM walls, from outside to inside, consisted of a novel triple glass (NTG), an air gap, PCM plasterboards, brick, and insulation, as shown in Figs. 1 and 2. The test room was equipped with electrical heaters keeping the indoor air at a comfortable temperature. The electrical heaters were considered a primary heating system, while the PCM walls were considered a secondary or assistant heating system for the test room.

The middle layer of the glass in the NTG was Prismasolar® glass (Lamberts Glass GmbH & Co. KG, 2010) that transmits solar rays that have a lower angle of incidence and reflects solar rays that have a higher angle of incidence (Fig. 2). The incident angle of solar rays is lower in the winter and higher in the summer; therefore, the majority of the sunlight incident on the NTG is transmitted in the winter and reflected in the summer by the Prismasolar® glass. Thus, the amount of thermal energy stored in the PCM plasterboards was lower in the summer and higher in the winter.

The south façade of the test room consisted of two PCM walls for simultaneously testing the performance of two PCMs with different melting temperatures. The PCM plasterboards shown in Fig. 1 included Rubitherm® GR35 and GR41 as the PCM. Rubitherm® GR is a heat storage granulate that uses paraffin as a PCM within a secondary supporting structure to ensure that the PCM, when in liquid form, does not leak out of the granulate. The granule size of GR35 and GR41 ranges between 1 and 3 mm (Rubitherm Technologies GmbH, 2010). The melting temperature ranges of GR35 and GR41 are 13 to 41 °C and 13 to 51 °C, respectively. Considering the typical supply air temperature in HVAC applications, which is 50 °C, the GR41 was used to provide warmer supply air from the GR41 PCM wall. In order to compare the thermal performance of the PCM walls, they were constructed identically and tested under the same conditions. Because there was no wall inside the test room separating the two PCM wall systems, as can be seen in Fig. 1, both of the PCM walls were exposed to the same indoor air conditions as well as the same outdoor conditions.

The PCM wall system operates on the following principles. In the winter, the solar radiation transmitting through the NTG was absorbed and stored by the PCM plasterboards (Fig. 2). The stored heat was then extracted and conveyed into the room via air circulation between the room and the air gap, caused by the fans (Fig. 1). The fan of the GR35 PCM wall was activated by another digital controller when the surface temperature of the GR35 PCM plasterboards exceeded 35 °C, which is the temperature of peak heat of fusion for GR35, the fan of the GR41 PCM wall was activated by a digital controller when the surface temperature of the GR41 PCM plasterboards exceeded 45 °C, which is the temperature of peak heat of fusion for GR41. The controllers deactivated the fans when the temperature of the plasterboards decreased to 25 °C. On the other hand, the electrical heaters were activated by a room thermostat in case the PCM walls did not provide enough energy to keep the indoor air at a comfortable temperature or there was no energy transfer from the PCM walls to the room. The electrical heaters were activated when the indoor air temperature fell below 20°C and deactivated when the indoor air temperature rose above 23 °C. In summer, the majority of the sun's rays were reflected by the NTG to prevent overheating.

The following parameters were measured and recorded on with a data acquisition system over a one-year period: solar radiation before and after the NTG, the inner and outer surface temperatures of the NTG, the surface temperature of the PCM plasterboards, the air temperatures at the inlet and outlet of the gap, the

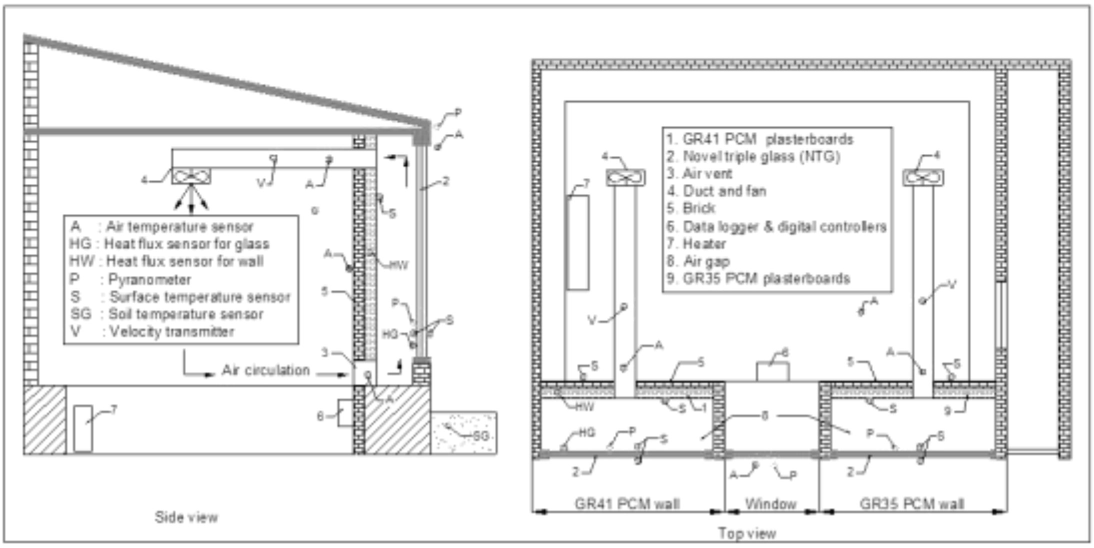

Figure 1. The layout of the test room

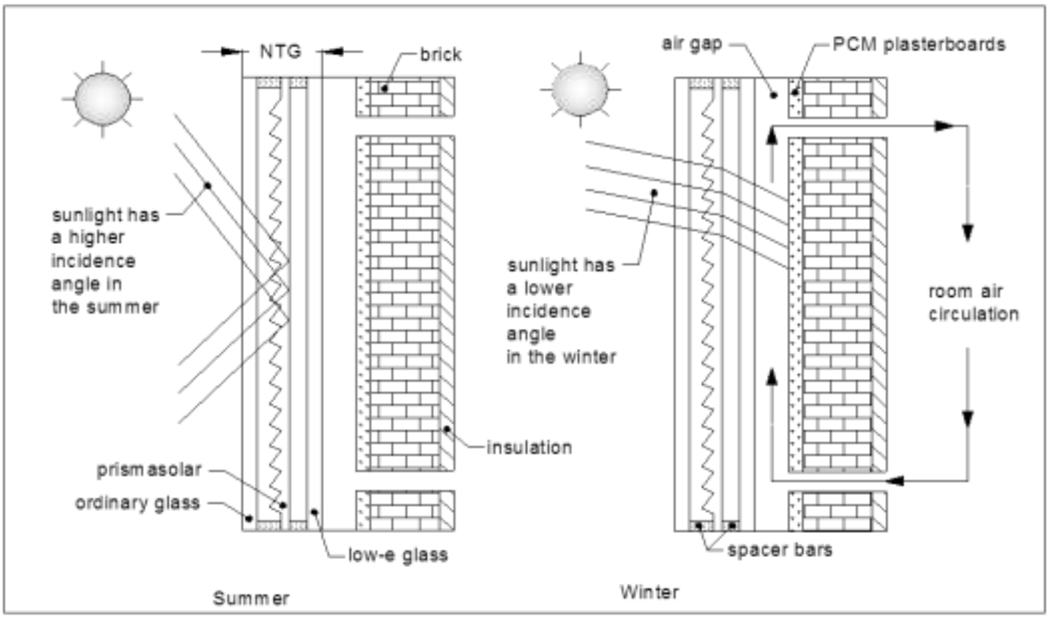

Figure 2. The working principle of the novel triple glass

indoor air temperature, the outdoor air temperature, the velocity of the circulation air, and the electric consumption of the heater (Fig. 1).

The test room was monitored continuously for a one-year period from October 2008 to October 2009, and the measured parameters were recorded at one-minute intervals by the data acquisition system. The recorded data was analysed on a monthly basis by employing the mathematical model described in Ref. (Kara and Kurnuç, 2012b) to determine the time-dependent variations of the parameters, including the SEG, solar transmittance of the NTG, and overall efficiency. The model is briefly presented below for the reader convenience.

The solar transmittance (ST) of the NTG was calculated as follows:

$$g(t) = \frac{I_i(t)}{I_t(t)} \quad (1)$$

where $I_i(t)$ is the solar radiation (W/m^2) incident on the NTG and $I_t(t)$ is the solar radiation transmitted through the NTG.

The heat rate (W) extracted from the wall and conveyed to the room was calculated as follows:

$$\dot{Q}_g(t) = \dot{m}_a c_{p,a}[T_{a,uv}(t) - T_{a,lv}(t)] \quad (2)$$

where $\dot{m}_a$ denotes the mass flow rate of the air circulated between the air gap and the test room, $c_{p,a}$ is the specific heat of the circulated air, and $T_{a,uv}(t)$ and $T_{a,lv}(t)$ are the instantaneous air temperatures at the upper and lower vents, respectively. The mass flow rate was calculated as follows:

$$\dot{m}_a = \rho_a V_m A_{c,d} \quad (3)$$

where V_m is the mean velocity of air for the cross-section of the duct and $A_{c,d}$ is the cross-sectional area of the duct. The daily solar energy (J/day) incident on the NTG was calculated as follows:

$$E_{i,d} = \int I_i(t) A_{s,NTG} dt \quad (4)$$

where $A_{s,NTG}$ is the surface area of the NTG.

The energy extracted from the PCM wall and conveyed to the test room, which is called the solar energy gain (SEG) (J/day) in this paper, was calculated on a daily basis as follows:

$$E_{g,d} = \int \dot{Q}_g(t) dt \quad (5)$$

The SEG (J/month) and the solar energy (J/month) incident on the NTG per month were calculated as follows:

$$E_{g,m} = \sum_{i=1}^{N} E_{g,d} \quad (6)$$

and

$$E_{i,m} = \sum_{i=1}^{N} E_{i,d} \quad (7)$$

where N is the number of days in each respective month.

The monthly mean overall efficiency of the PCM walls was calculated as follows:

$$\eta_{o,m} = \frac{E_{g,m}}{E_{i,m}} \quad (8)$$

An error analysis was completed using Kline and McClintock's method, as described by Holman (1994). The uncertainties for the monthly incident solar energy, the monthly SEG, and the overall efficiency were calculated to be ±6%, ±12%, and ±13.4%, respectively.

Theoretical Analysis

The monthly average daily radiation on the horizontal surface was calculated using weather data measured over a 10-year period between 1995 and 2005 in the city of Erzurum, where the test facility is available. The raw weather data were taken from the State Meteorological Affairs General Directorate of Turkey. The monthly average daily radiation on the south wall was then calculated using the monthly average daily data on the horizontal surface by employing Lui and Jordan's method as presented by Duffie and Beckman (1991). This method is briefly described below:

$$\overline{H}_T = \overline{H} \times \left(1 - \frac{H_d}{H}\right) \times \overline{R}_b + \overline{H}_d \times \left(\frac{1+\cos\beta}{2}\right) + \overline{H} \times r \times \left(\frac{1-\cos\beta}{2}\right) \quad (9)$$

where $\overline{H}_T$ is the monthly average daily radiation on the tilted surface, $\overline{H}$ is the monthly average daily radiation on the horizontal surface, $\overline{H}_d$ is the diffuse component of $\overline{H}$, r is the diffuse reflectance of the surroundings, and $\overline{R}_b$ is the ratio of the average daily beam radiation on the tilted surface to that on a horizontal surface for the month, which is given by

$$\bar{R}_b = \frac{\cos(\phi-\beta)\cos\delta\sin\omega'_s + \left(\frac{\pi}{180}\right)\omega'_s\sin(\phi-\beta)\sin\delta}{\cos\phi\cos\delta\sin\omega_s + \left(\frac{\pi}{180}\right)\omega_s\sin\phi\sin\delta} \tag{10}$$

The variables ω'_s and ω_s are the sunset hour angles for the tilted and horizontal surfaces for the mean day of the month, and ω'_s is given by

$$\omega'_s = \min\begin{bmatrix}\cos^{-1}(-\tan\phi\tan\delta) \\ \cos^{-1}(-\tan(\phi-\beta)\tan\delta)\end{bmatrix} \tag{11}$$

where "min" indicates the smaller of the two items in the brackets, β is the slope angle of a surface, δ is the declination angle for the mean day of the month, and ϕ is the latitude of the location.

The solar energy incident on the NTG, $E_{i,m}$ and SEG provided by the PCM walls, $E_{g,m}$ were calculated on a monthly basis as follows:

$$E_{i,m} = \bar{H}_T \times A_s \times N \tag{12}$$

and

$$E_{g,m} = \eta_{o,m} \times E_{i,m} \tag{13}$$

where $\eta_{o,m}$ is the monthly average overall efficiency of the PCM wall calculated by using Eq. (8) and $A_{s,NTG}$ is the surface area of the NTG.

The monthly heat load $(E_{h,m})$ of the test room was calculated using the method given by the Institute of Turkish Standards (Anonymous, 2008), which is briefly described below. The monthly heat load, $E_{h,m}$ (J/month) is the difference between the total heat loss and the total heat gain of the building, which was calculated as follows:

$$E_{h,m} = [H(T_{i,a} - T_{o,a,m}) - f(\dot{Q}_i + \dot{Q}_s)] \times t \tag{14}$$

where $T_{i,a}$ is the indoor air temperature (K), $T_{o,a,m}$ is the monthly mean outdoor air temperature (K), t is the period of one month in seconds, $\dot{Q}_i$ is the inside heat gain (W) caused by human bodies and the facilities in the building such as lighting and electrical equipment, $\dot{Q}_s$ is the solar heat gain (W) through the windows, and f is the correction factor for the heat gains. The specific heat loss, H (W/K), in Eq. (14) is given by

$$H = H_c + H_v \tag{15}$$

where H_c is the specific heat loss via heat conduction and H_v is the specific heat loss via ventilation. The specific heat loss via heat conduction is given by

$$H_c = \sum(AU + Ik) \tag{16}$$

where A is the heat transfer area and U is the overall heat transfer coefficient (W/m^2·K) for the building components, such as the exterior walls and ceiling. The second term in Eq. (16) considers the heat loss due to conduction through the heat bridges such as through the balcony. Here, I is the characteristic length (m) and k is the heat conduction coefficient (W/m·K) of the heat bridge. The specific heat loss via ventilation is given as follows:

$$H_v = \rho c_p n_v V_v \tag{17}$$

where ρ and c_p are the density and the specific heat of the air, n_v is the number of air changes per hour (h^{-1}), and V_v is the volume ventilated. The ratio of solar energy gain (RSEG) was calculated by dividing the solar energy gain (SEG) provided by the PCM wall to the heat load of the test room:

$$RSEG = E_{g,m} / E_{h,m} \tag{18}$$

RESULTS AND DISCUSSION

Energy Evaluation Based on The Experimental Analysis

Thermal characteristics of GR35 and GR41 were tested by differential scanning calorimetry (DSC) in the Central Laboratory of Middle East Technical University (2012). The testing instrument was Perkin Elmer Diamond DSC, which has the accuracy of ±0.1 ºC and < ±1% for temperature and calorimeter, respectively. The heat of fusion of GR35—that is, the latent heat storage capacity—in the temperature range of 13 to 41 ºC is 41 kJ/kg, and the temperature at the peak heat of fusion is 34 ºC. On the other hand, the heat of fusion of GR41 in the temperature range of 13 to 51 ºC is 55 kJ/kg, and the temperature at the peak heat of fusion is 45 ºC.

The energy calculations based on experimental data were carried out by using Eqs. (1) through (8), and the main results are briefly shown in Fig. 3 through 5. However, comprehensive energy evaluations are available in references (Kara and Kurnuç, 2012a; Kara and Kurnuç, 2012b). Fig. 3 shows the solar energy gains provided by the PCM walls and solar energy incident on the NTG of a PCM wall. The SEG from the GR35 wall was higher than that of the GR41 wall. Fig. 4 shows monthly mean overall efficiency of the PCM walls. The monthly mean overall efficiency of the PCM walls varied between 20 and 30% from October to March. The overall efficiency of the GR35 wall was slightly higher than that of GR41 wall. On the other hand, the difference between the temperatures of the supply air at the upper vents of the GR35 and GR41 walls was insignificant (Kara and Kurnuç, 2012b).

Considering Fig. 3 and 4, GR35 was the more efficient PCM in this study because its energy storage temperature was lower; a low storage temperature led to lower absorber temperatures and lower heat loss, and thus to better efficiency. In other words, the high-energy storage temperature of GR41 resulted in a lower efficiency due to higher heat losses. The solar energy gain (Fig. 3) and the monthly mean overall efficiency (Fig. 4) decreased in March and were zero in April and May because the solar transmittance (ST) decreased dramatically after March 21 (Fig. 5). The ST varied between 0.45 and 0.55 from October to February; it then decreased below 0.25 after March 21 and varied over a range between 0.20 and 0.25 from April to the end of May.

The NTG sufficiently fulfilled its design goal because the ST decreased by nearly 100% during the summer compared with the winter. Reducing the energy storage during the summer period was the goal during the design stage to avoid overheating, as was mentioned in experimental work section.

Energy Evaluation Based on The Theoretical Analysis

The solar energy incident on the NTGs and the solar energy gain provided by the PCM walls were calculated from Eqs. (9) through (13). The solar energy gains in Fig. 6 were calculated by assuming that PCM GR35 or PCM GR41 is used alone within the entire south wall of the test room; that is, only GR35 or GR41 is used in both of the PCM walls. Fig. 6 also shows the monthly variation of the heat load of the test room, which was calculated from Eqs. (14) through (17). Ignoring the very small heat load that appeared in June and September, the months of October, November, December, January, February, March, April, and May can be considered as the heating period for Erzurum, where annual the heating degree-days is 4,856. Thus, the months of June, July, August and September were excluded because the analysis covers only the heating period. It can be inferred from Figs. 5 and 6 that the ST decreased to its minimum value approximately two months before the end of the heating season in Erzurum. Therefore, the current NTG is not suitable for cities where the number of annual heating degree-days is around 4,856. The NTG is more suitable for the cities

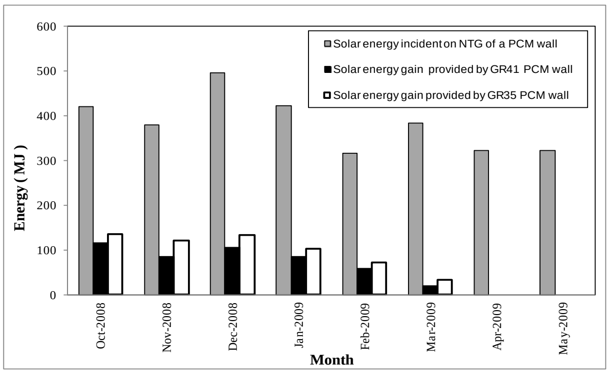

Figure 3. Monthly solar energy gain provided by PCM walls and monthly solar energy incident on a PCM wall evaluated experimentally

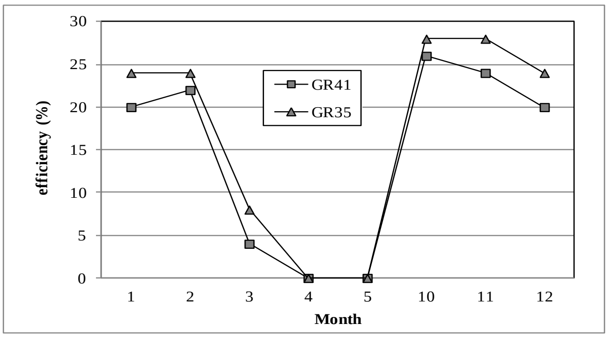

Figure 4. Monthly mean overall efficiency of the PCM walls calculated experimentally

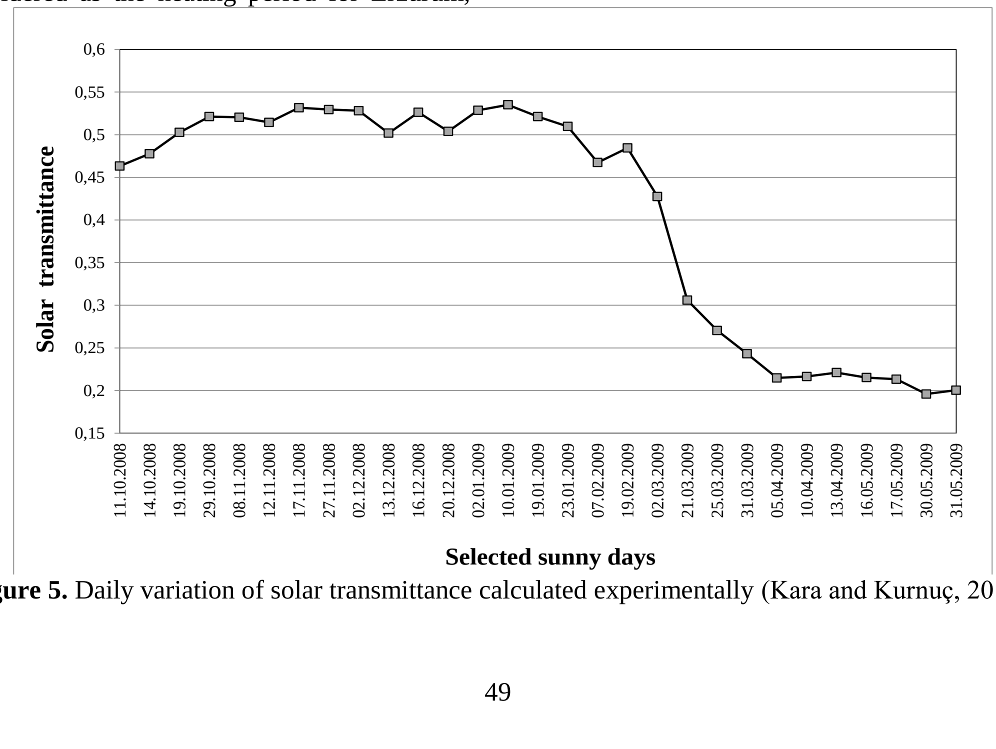

Figure 5. Daily variation of solar transmittance calculated experimentally (Kara and Kurnuç, 2012)

where the number of annual heating degree-days is around 1,450. On the other hand, the amount of total incident solar energy is lower than the heat load of the test room in December, January, February, and March (Fig. 6). This indicates that if all of the incident solar energy was gained, it still would not be sufficient to overcome the heating load of the test room.

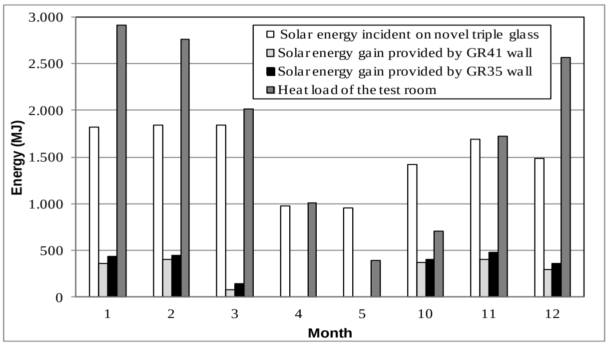

Figure 6. Energy balance of the test room evaluated theoretically

The ratio of solar energy gain (RSEG) calculated from Eq. (18) indicates the fraction of the monthly heat load provided by the PCM wall; in other words, it indicates the benefit of using the PCM wall on south façade. Fig. 7 shows the monthly variation of the RSEG. According to Fig. 7, the RSEG of the GR35 PCM wall is 57% in October, 27% in November, 14% in December, 15% in January, 16% in February, 7% in March, and 0% in April and May. The RSEGs of the GR41 PCM wall are slightly lower than those of the GR35 PCM wall because the monthly mean overall efficiency of the GR35 PCM wall was higher than that of the GR41 PCM wall, as shown in Fig. 4. The annual RSEGs of the GR35 PCM wall and the GR41 PCM wall were calculated as 16% and 14%, respectively.

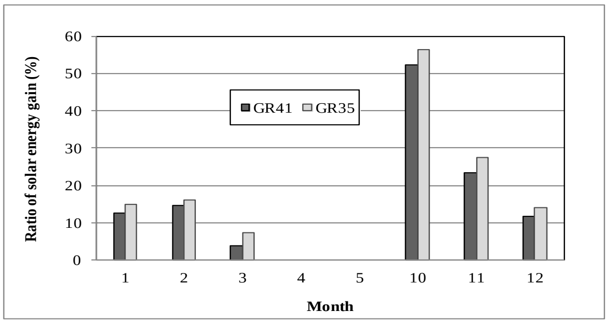

Figure 7. The ratio of solar energy gain (RSEG) calculated theoretically

CONCLUSION

A test room with PCM walls was built to investigate the thermal performance of the PCM walls. The PCM walls are made of brick walls, plasterboards containing PCMs, and novel triple glass. The test room was monitored over a one-year period, and the thermal performances of the walls were determined both experimentally and theoretically.

The experimental analysis showed that the GR35 wall performed better than the GR41 wall because the energy storage temperature of GR35 was lower. The high-energy storage temperature of GR41 resulted in lower efficiency due to higher heat losses. The ST of the NTG decreased nearly 100% during the summer as compared to winter. The NTG reduced the energy storage in the PCM wall and prevented the PCM wall overheating in summer.

The theoretical analysis showed that the RSEG of the GR35 PCM wall is 57% in October, 27% in November, 14% in December, 15% in January, 16% in February, 7% in March, and 0% in April and May. The mean RSEG of the GR35 PCM wall was calculated as 16% on an annual basis; that is, the GR35 PCM wall can provide 16% of the annual heat load of the test room. In the case in which GR41 is used as a PCM, the monthly RSEGs are slightly lower than those of a GR35 PCM wall.

Acknowledgments

This study is supported by the Scientific and Technological Research Council of Turkey (TUBITAK) under project number 107M154

REFERENCES

Anonymous, 2008, *Thermal insulation requirements for buildings, TS 825*, The Institute of Turkish Standards, Ankara.

Baetens R., Jelle B.P. and Gustavsen A., 2010, Phase change materials for building applications: A state-of-the-art review, *Energy and Buildings*, 42, 1361–1368.

Cabeza L.F., Castellon C., Nogues M., Medrano M., Leppers R. and Zubillaga O., 2007, Use of microencapsulated PCM in concrete walls for energy savings, *Energy and Buildings*, 39, 113–119.

Castell A., Martorell I., Medrano M., Perez G. and Cabeza L.F., 2010, Experimental study of using PCM in brick constructive solutions for passive cooling, *Energy and Buildings*, 42, 534–540.

Castellón C., Medrano M ., Roca J., Cabeza L.F., Navarro M.E., Fernández A.I., Lázaro A. and Zalba B., 2010, Effect of microencapsulated phase change material in sandwich panels, *Renewable Energy*, 35, 2370–2374.

Central Laboratory of Middle East Technical University, 2012, http:// www.merlab. metu.edu.tr/en/

Cerón I., Neila J. and Khayet M., 2011, Experimental tile with phase change materials (PCM) for building use, *Energy and Buildings*, 43, 1869–1874.

Chan A.L.S., 2011, Energy and environmental performance of building facades integrated with phase change material in subtropical Hong Kong, *Energy and Buildings*, 43, 2947–2955.

Diaconu B.M. and Cruceru M., 2010, Novel concept of composite phase change material wall system for year-round thermal energy savings, *Energy and Buildings*, 42, 1759–1772.

Duffie J.A. and Beckman W.A., 1991, *Solar Engineering of Thermal Processes* (Second Ed.), John Wiley & Sons Inc., New York.

Hauer A., Mehling H., Schossing P., Yamaha M., Cabeza L., Martin V. and Setterwall F., 2002, *IEA, ECES IA Annex 17, Final Report*,. Retrieved 2010 from http://www.iea-eces.org/annexes/completed-annexes.html.

Holman J.P., 1994, *Experimental Methods for Engineers* (Sixth Ed.), McGraw-Hill, Singapore.

Kara Y.A. and Kurnuç A., 2012a, Performance of coupled novel triple glass unit and PCM wall, *Applied Thermal Engineering*, 35, 243–246.

Kara Y.A. and Kurnuç A., 2012b, Performance of coupled novel triple glass and phase change material wall in the heating season: an experimental study, *Sol. Energy*, 86, 2432–2442.

Khudhair A.M. and Farid M.M., 2004, A review on energy conversation in building applications with thermal storage by latent heat using phase change materials, *Energy Conversion and* Management, 45, 263–275.

Kuznik F., Virgone J. and Johannes K., 2011, In-situ study of thermal comfort enhancement in a renovated building equipped with phase change material wallboard, *Renewable Energy*, 36, 1458–1462.

Lamberts Glass GmbH & Co. KG, 2010. www.lamberts.info

Lin K., Zhang Y., Xu X., Di H., Yang R. and Qin P., 2004, Modeling and simulation of under-floor electric heating system with shape-stabilized PCM plates, *Building and Environment*, 39, 1427–1434.

Lin K., Zhang Y., Xu X., Di H., Yang R. and Qin P., 2005, Experimental study of under-floor electric heating system with shape-stabilized PCM plates, *Energy and Buildings*, 37, 215–220.

Liu H. and Awbi H.B., 2009, Performance of phase change material boards under natural convection, *Building and Environment*, 44, 1788–1793.

Pasupathy A., Velraj R. and Seeniraj R.V., 2008, Phase change material-based building architecture for thermal management in residential and commercial establishments, *Renewable and Sustainable Energy Reviews*, 12, 39–64.

Rubitherm Technologies GmbH, 2010. www.rubitherm.com

Sharma A., Tyagi V.V., Chen C.R. and Buddhi D., 2009, Review on thermal energy storage with phase change materials and applications, *Renewable and Sustainable Energy Reviews*, 13, 318–345.

Tyagi V.V. and Buddhi D., 2007, PCM thermal storage in buildings: A state of art, *Renewable and Sustainable Energy Reviews*, 11, 1146–1166.

Zhang C., Chen Y., Wu L. and Shi M., 2011, Thermal response of brick wall filled with phase change materials (PCM) under fluctuating outdoor temperatures, *Energy and Buildings*, 43, 3514–3520.

Zhang Y., Zhou G., Lin K., Zhang Q. and Di H., 2007, Application of latent heat thermal energy storage in buildings: State-of-the-art and Outlook, *Building and Environment*, 42, 2197–2209.

Zhang Y.P., Lin K., Yang R., Di H.F. and Jiang Y., 2006, Preparation, thermal performance and application of shape-stabilized PCM in energy efficient buildings, *Energy and Buildings*, 38, 1262–1269.

Zhou G., Zhang Y., Lin K. and Xiao W., 2008, Thermal analysis of a direct-gain room with shape-stabilized PCM plates, *Renewable Energy*, 33, 1228–1236.

Zhou G., Zhang Y., Zhang Q., Lin K. and Di H., 2007, Performance of a hybrid heating system with thermal storage using shape-stabilized phase-change material plates, *Applied Energy*, 84, 1068–1077.

Yusuf Ali Kara is an Associate Professor in the Department of Mechanical Engineering, University of Atatürk, Turkey. He received his Ph.D. in 1999 from Atatürk University. His main research interests are heat pumps, heat exchangers, and renewables. He has published 7 articles in international journals.

Aslıhan KURNUÇ was born in Erzurum in 1980. She graduated from Ataturk high school in 1997. In 2001 she received her BS degree in mechanical engineering from Ataturk University. She obtained her Ph.D. degree in the same field from Ataturk University in 2010. Currently she is an assistant professor at Erzincan University Department of Mechanical Engineering. Her current research interest is on renewable energy.